OPEN ACCESS Freely available online

PLOS ONE

Escitalopram Decreases Cross-Regional Functional Connectivity within the Default-Mode Network

Vincent van de Ven[1]*, Marleen Wingen[2], Kim P. C. Kuypers[2], Johannes G. Ramaekers[2], Elia Formisano[1]

1 Department of Cognitive Neuroscience, Faculty of Psychology and Neuroscience, Maastricht University, Maastricht, The Netherlands, **2** Department of Neuropsychology and Psychopharmacology, Faculty of Psychology and Neuroscience, Maastricht University, Maastricht, The Netherlands

Abstract

The default-mode network (DMN), which comprises medial frontal, temporal and parietal regions, is part of the brain's intrinsic organization. The serotonergic (5-HT) neurotransmitter system projects to DMN regions from midbrain efferents, and manipulation of this system could thus reveal insights into the neurobiological mechanisms of DMN functioning. Here, we investigate intrinsic functional connectivity of the DMN as a function of activity of the serotonergic system, through the administration of the selective serotonin reuptake inhibitor (SSRI) escitalopram. We quantified DMN functional connectivity using an approach based on dual-regression. Specifically, we decomposed group data of a subset of the functional time series using spatial independent component analysis, and projected the group spatial modes to the same and an independent resting state time series of individual participants. We found no effects of escitalopram on global functional connectivity of the DMN at the map-level; that is, escitalopram did not alter the global functional architecture of the DMN. However, we found that escitalopram decreased DMN regional pairwise connectivity, which included anterior and posterior cingulate cortex, hippocampal complex and lateral parietal regions. Further, regional DMN connectivity covaried with alertness ratings across participants. Our findings show that escitalopram altered intrinsic regional DMN connectivity, which suggests that the serotonergic system plays an important role in DMN connectivity and its contribution to cognition. Pharmacological challenge designs may be a useful addition to resting-state functional MRI to investigate intrinsic brain functional organization.

Citation: van de Ven V, Wingen M, Kuypers KPC, Ramaekers JG, Formisano E (2013) Escitalopram Decreases Cross-Regional Functional Connectivity within the Default-Mode Network. PLoS ONE 8(6): e68355. doi:10.1371/journal.pone.0068355

Editor: Satoru Hayasaka, Wake Forest School of Medicine, United States of America

Received July 28, 2012; **Accepted** May 29, 2013; **Published** June 27, 2013

Funding: This study was in part financially supported by grants from pharmaceutical industries (Organon, Pierre Fabre, FAES pharma, GSK) and the European Committee to JR, and by grants from the Netherlands Organisation for Scientific Research (NWO) to VV, JR and EF. The funders had no role in study design, data collection and analysis, decision to publish, or preparation of the manuscript.

Competing Interests: Funders included the commercial sources Organon, Pierre Fabre, FAES Pharma and GSK. There are no patents, products in development or marketed products to declare. This does not alter the authors' adherence to all the PLOS ONE policies on sharing data and materials.

* E-mail: v.vandeven@maastrichtuniversity.nl

Introduction

The brain's functional organization includes a network of medial frontal and parietal cortex and hippocampal areas [1–4]. This network has been termed the "default mode" network (DMN) [5] because it typically shows increased metabolic activity during resting baseline compared to periods of goal-directed cognitive behaviour. The DMN is thought to play a role in a number of cognitive and affective behaviours, including social and self-referential perception [6–8], internal mental representation [9] and memory [4,10–13]. Furthermore, the DMN may be involved in the neuropathology of a number of clinical disorders. For example, memory impairments in Alzheimer's Disease (AD) may be associated with impaired hippocampal connectivity with the remainder of the DMN [14–16]. Also, impaired medial frontal, parietal or temporal connectivity may respectively contribute to affective processing deficits in major depression (MD) [17,18], and psychotic symptoms in schizophrenia [19,20].

The DMN has also been investigated in many functional magnetic resonance imaging (fMRI) studies that measured intrinsic brain activity, during resting-states in which participants refrained from specific task performance [1–3,21,22]. The fMRI signal measured during such resting states are likely to have a neurophysiological source [23–25], and may influence or facilitate on-line goal-directed cognitive performance [10,26–28]. In this sense, resting-state measurements provide a simple opportunity to study the brain's functional organization at relatively low cognitive demands for the patients, which makes it an appealing paradigm for clinical research.

However, a more detailed neurobiological understanding of DMN functionality is currently lacking. One possible method to investigate the DMN in humans is to measure the DMN's intrinsic organization as a function of the activity of neurotransmitter systems. Previously, fMRI has been used to measure brain activity after administration of pharmacological agents that are used to manipulate the activity of particular neurotransmitter systems, compared to placebo (pharmacological fMRI or ph-fMRI). These ph-fMRI studies showed regional differential responses of brain activity after administration of pharmacological agents, compared to placebo [29,30], as well as regionally specific interactions between agent and task performance [31–34]. Previously, we showed that the selective serotonin reuptake inhibitor (SSRI) escitalopram decreased brain activity in thalamic and medial and lateral prefrontal cortical regions, compared to placebo, during the execution of a vigilance task [34]. Escitalopram did not change

behavioral performance, but did show a significant decrease in self-reported alertness.

Recently, pharmacological challenge has also been conducted in resting state fMRI measurements in healthy participants. So far, these studies provided little or no evidence of changes in DMN connectivity after administration of alcohol [35,36] or morphine [36], compared to placebo. However, one study reported that the dopamine agonist L-Dopa decreased functional connectivity of medial DMN regions [37]. Carhart et al. recently showed decreased functional coupling between medial frontal and parietal regions of the DMN after intake of psilocybin [38], a psychedelic compound, which could be associated with increased serotonergic activity [39]. Finally, Northoff and colleagues reported that GABA concentrations in ventromedial prefrontal cortex predicted amount of deactivations in this region of cortex [40]. These findings, thus, indicate that DMN functionality could depend on the interaction between multiple neurotransmitter systems, and that resting-state ph-fMRI may be very suitable to probe this mechanism.

In the current study, we analyzed the effects of the SSRI escitalopram on the intrinsic functional connectivity of the DMN. The serotonergic (5-hydroxytryptamine, 5-HT) neurotransmitter system may play a role in the intrinsic functional dynamics of the DMN for a number of reasons. Ascending serotonergic pathways from the midbrain raphe nucleus project onto many cortical and subcortical limbic system areas, including hippocampal structures, amygdala and cingulate cortex regions, which are part of the DMN functional architecture [1,2,5]. Serotonin may play an important role in cognitive functioning in healthy participants [41,42], such as modulating levels of alertness or sustained attention [43], or long-term memory [44,45]. Furthermore, pharmacological brain imaging studies showed that administration of serotonergic agents to healthy participants altered brain activity in cingulate areas [29,30] and hippocampus [29]. Specifically, escitalopram has been found to decrease brain activity in medial cortical and hippocampal areas during task executions [31,33,34]. These changes in brain activity are very likely to impact the functional integration of these brain areas within the DMN, which may in turn affect cognitive processing and contribute to pathological manifestations. For example, serotonin dysfunctions have been associated with symptomatology and cognitive impairments in MD [43] [46], as well as in AD [46] and schizophrenia [47]. In MD, selective serotonin reuptake inhibitors (SSRIs), which increase 5-HT synaptic availability or functioning, alleviate affective symptoms and improve memory performance and other cognitive functions (see [43] for review).

We previously obtained two resting-state timeseries of healthy individuals as part of a placebo-controlled, within-subject ph-fMRI study that investigated the effects of escitalopram on the neural correlates of vigilance [34]. We hypothesized that escitalopram, compared to placebo, decreased intrinsic functional connectivity of the DMN. We tested the hypothesis at the level of global connectivity (i.e., at the map-level), and at the level of local (regional) connectivity, as these two levels of analysis may provide related but distinct information about functional network dynamics [48,49]. We used a dual regression approach [36,49,50], in which we first quantified intrinsic DMN functional connectivity during placebo and drug conditions of the first resting-state using group spatial independent component analysis (sICA) [51,52], and then dual-regressed the spatial modes onto the timeseries of the first and the second resting state segment of individual participants. The effect of escitalopram on global DMN connectivity was assessed using a voxel-by-voxel analysis, and the effect on local connectivity using a pairwise region-of-interest approach.

Methods

Subjects

Ten healthy volunteers (5 females), mean age (se) 26.3 (2.46) were recruited. Recruited participants were free of a history of previous use of antidepressant medication (recruitment procedures and in- and exclusion criteria are described elsewhere [34]). The study was approved by the medical ethics committee of Maastricht University and the Maastricht Academic Hospital's Board of Directors, and was carried out in accordance with the World Medical Association's *Declaration of Helsinki* (Edinburgh, 2000). Written informed consent was obtained from each volunteer prior to participation in the study.

Design and Treatment

The resting state measurements were obtained as part of a previous study that measured the effects of escitalopram on vigilance [34]. Here, we briefly reiterate the experimental design and pharmacological parameters. A more elaborate description can be found in our previous text.

The study was conducted according to a double-blind, placebo controlled, 2-way cross-over design. Complete balancing of the treatments led to two treatment orders that were randomly assigned to the participants. Treatments consisted of escitalopram (20 mg) and placebo administered at 2 different test days separated by a wash-out period of at least 7 days.

On the days of measurement, participants arrived at 9.00 a.m. at the laboratory, filled out an informed consent concerning scanning procedures, received a standard breakfast and completed a sleep quality questionnaire. They received the treatment capsule containing either escitalopram or placebo at 9.30 a.m. Oral administration of escitalopram reaches the maximum concentration in blood (Cmax) within 3–4 hours, and has a half-life elimination of 27–32 hours [53]. Participants were then seated for the next hours in a secluded waiting room in order to wait for escitalopram to reach Cmax. At noon participants received a standard light lunch, followed by a self-report assessment of alertness, contentedness and calmness [54] (visual analogue scales [VAS]; range, 0–100; 0 = low, 100 = high). As reported previously [34], participants reported significantly lower Alertness ratings after escitalopram administration (Alertness = 67.0) compared to placebo (Alertness = 81.4; $T(9) = -4.6$, $P = 0.001$). Ratings on contentedness and calmness did not significantly differ between the two drug conditions. Scanning and testing took place at 13.30 p.m., i.e. 4 hrs after drug intake, till 14.15 p.m. Participants were not allowed to consume alcohol 24 hours prior to testing and caffeine-containing beverages 4 hours prior to the start of the measurement day.

FMRI Data Acquisition

Measurements were acquired using a 3T Siemens Allegra MR scanner. A T1-weighted anatomical scan was acquired for each participant using a 3D modified driven equilibrium fourier transform (MDEFT) sequence (176 slices; in-plane resolution, 1 mm^2). A T2*-weighted functional measurement was acquired using an echo-planar image (EPI) pulse sequence (1,316 whole-brain volumes; 32 slices; slice thickness, 3.5 mm; no slice gap; flip angle 90°; TR/TE, 2,000/30 msec; in-plane resolution, 3.5×3.5 mm^2, matrix size, 64×64) and interleaved slice sampling. The complete timeseries comprised a first resting state measurement (volumes 1–210), followed by the vigilance task (211–1106), and ended with a second resting state measurement (1107–1316). During the resting measurement, participants fixated

their gaze on a fixation cross, and no additional stimulus or task was presented.

Data Preprocessing

The first two volumes of each complete time series were discarded because of saturation effects. Preprocessing of the functional images was done using BrainVoyager QX version 1.6 [55], and included slice time correction, head motion correction, spatial smoothing (Gaussian kernel with full-width-at-half-maximum of 6 mm), and linear trend removal of time courses and high pass temporal filtering of 5 cycles per time course ($\sim$ 0.0019 Hz). Individual anatomical datasets were spatially normalized to a standardized 3-dimensional (3D) space [56]. Individual functional images were co-registered and normalized to the anatomical data, and resampled to a voxel size of $3\times3\times3$ mm^3. The standardized anatomical images of the participants were averaged and a group-based volume mask was created that tagged voxels belonging to cerebral and cerebellar matter (selecting 50,381 voxels, $\approx$ 47% of total volume), and excluded voxels belonging to ventricular space or tissue outside of the brain. For the first and second resting state segments, RS1 and RS2, we dropped the respective last and first four volumes in order to prevent any effects of task on- or offset. Thus, each resting-state segment included 204 timepoints.

Functional Connectivity Analysis

Intrinsic functional connectivity was estimated for the two resting-state segments of the time series (RS1 and RS2). We used spatial independent component analysis (sICA) to decompose the RS1 timeseries of all participants, but separately for escitalopram and placebo runs, into a set of 40 spatial modes. For this analysis, RS1 timeseries were normalized and concatenated across time, resulting in an aggregated data matrix of 2,040 volumes ($=10$ participants$\times$204 volumes) by 50,381 voxels for the escitalopram (i.e., RS1E) and placebo (RS1P) runs. FastICA [57] was used to spatially decompose each aggregate data matrix into 40 independent components using the symmetric decomposition option. Initial dimension reduction was performed using principal component analysis (PCA). Details of the spatial ICA decomposition in fMRI are described elsewhere [22,51,52,58,59]. We used a spatial template of the posterior cingulate cortex (PCC) from an independent study [22] (center of mass [x, y, z] = -1, -47, 24; size = 13,319 mm^3) to label and select one DMN functional connectivity map in each decomposition according to the highest absolute correlation with the spatial template (RS1E $\max(|r|) = 0.43$; RS1P $\max(|r|) = 0.42$).

Following the dual-regression analysis scheme [36,60,61], we first spatially regressed the (Z-normalized) spatial modes of the RS1E and RS1P decompositions onto the RS1 and RS2 timeseries of the respective drug condition. Thus, the spatial modes were applied to the data from which they were estimated (i.e., RS1), and to a second dataset of the same participants (RS2). This step resulted in a set of temporal profiles of the spatial modes. In the second step, we temporally regressed the temporal profiles onto the complete functional runs.

We then analysed the effects of escitalopram on DMN connectivity at the map-level, which assesses global (multivariate) connectivity, and at the regional-level, which assesses local (pairwise) connectivity. The two levels of analysis can provide related but distinct information about the effects of escitalopram on network connectivity [48,49]. To assess map-level effects of escitalopram we investigated the voxel-by-voxel results of the DMN temporal profiles, comparing DMN connectivity between the two drug conditions. To assess regional effects of escitalopram on DMN connectivity, we followed a region-of-interest (ROI) approach, in which ROIs were obtained from a one-sample t-test map of the functional connectivity values across all conditions and timeseries. From the ensuing ROIs we sampled timeseries from DMN regions and removed effects of non-DMN temporal profiles (obtained from the first dual-regression step), and a number of fMRI covariates [3,62–64] including head movement, fMRI signal from the ventricles and from white matter, and signal oscillations at a frequency above 0.1 Hz (using pairs of discrete sines and cosines). The corrected ROI timeseries were then segmented according to the RS1 and RS2 time windows, Z-normalized and pair-wise correlated using the Pearson correlation coefficient. Correlation coefficients r were then transformed to normality using Fisher's Z normalization for further analysis using repeated measures ANOVA (RMANOVA) with within-subject factors Drug (Escitalopram, Placebo) and Time (RS1, RS2), and their Drug x Time interaction term. Pairwise ROI connections that showed a significant effect on at least one of these factors were considered for post-hoc analysis, which included paired-sample t-tests ($df = 9$). Functional connectivity estimation and statistical analysis of the results were performed in Matlab (MathWork, Inc.), in which we used an adapted version of the RMANOVA implementation written by Trujillo-Ortiz et al. [65]. Correction for multiple pairwise comparisons was performed using a false-discovery rate (FDR) of $q = 0.05$ [66].

To define DMN ROIs for the regional connectivity analysis, we averaged the spatial maps from the second dual-regression step across the two resting states and the two drug conditions, and calculated a mass-univariate one-sample t-test map, which was thresholded using $q(FDR) = 0.05$ and minimum cluster size of 270 mm^3, corresponding to a cluster-level threshold alpha = 0.05, as estimated by a simulation procedure (1,000 Monte Carlo simulations) of the statistical map that is based on its estimated spatial smoothness [55,67]. This procedure resulted in seven ROIs, which included anterior cingulate cortex/ventromedial prefrontal cortex (ACC), posterior cingulate cortex/precuneus (PCC), left and right hippocampal and parahippocampal complex (LPHC and RPHC), left and right inferior parietal cortex/posterior part of the superior temporal gyrus (LIPC and RIPC), and left middle frontal gyrus (LMFG). Pairwise correlations resulted in $\frac{N_{ROI}\cdot(N_{ROI}-1)}{2} = 21$ unique correlations per resting state, drug condition and participant. **Table 1** lists the ROI sizes in mm^3 and Talairach coordinates.

Results

The effect of escitalopram was first assessed at the map level using a mass-univariate, voxel-by-voxel RMANOVA of the dual-

Table 1. ROI details. ROI, region-of-interest; k, voxel cluster size in mm^3; x,y,z, Talairach coordinates in mm.

ROI	k	x	y	z
PCC	41500	0	−51	25
RIPC	9338	44	−59	22
LIPC	6136	−44	−59	20
RPHC	1547	21	−14	−18
ACC	1287	1	53	6
LPHC	846	−22	−11	−18
RMFG	649	23	21	48

doi:10.1371/journal.pone.0068355.t001

regression estimates for functional connectivity. **Figure 1** shows the spatial DMN maps obtained from the aggregated sICA of the RS1 segment of the escitalopram (**Fig. 1, upper row**) and placebo runs (**Fig. 1, bottom row**). The sICA results were used as input to the dual-regression analysis to estimate global functional connectivity of the DMN for the escitalopram and placebo functional timeseries of RS1 and RS2. The ensuing results were analysed using a voxel-by-voxel RMANOVA, and results were thresholded using q(FDR) = 0.05 and a minimum cluster size of 270 mm^3. The analysis yielded no significant effects of Drug, Time or the Drug x Time interaction effect.

The effect of escitalopram on regional connectivity between the seven DMN ROIs was assessed using a pairwise ROI approach. ROIs included ACC, PCC, LPHC, RPHC, LIPC and RIPC (see **Table 1** for further details). **Figure 2** shows the color-coded F-values for the RMANOVA within-subject factors of Drug (**Fig. 2A**) and Time (**Fig. 2B**), and the Drug x Time interaction term (**Fig. 2C**). After FDR correction for multiple comparisons of pairwise ROI correlations, seven functional connections showed a significant effect of Drug (marked by asterisk in **Fig. 2A**). The pairwise connections included PCC-RIPC, PCC-RPHC, RIPC-RPHC, LIPC-RPHC, ACC-RPHC and RPHC-RMFG. Functional connections showed no significant effects of Time or of the interaction between Drug and Time, which suggests that escitalopram-related changes in functional connectivity between DMN ROIs was similar for both resting states RS1 and RS2. Post-hoc paired-sample t-tests of the seven connections showed that escitalopram reduced pairwise functional connectivity strength, compared to Placebo, in both RS1 and RS2. Barplots of **Figure 3A** show the respective means of the connectivity values for the escitalopram (grey bars) and Placebo condition (black bars), for both resting states RS1 and RS2, and **Table 2** lists the statistical values of the comparisons. We did not observe any significant effect of Time or the Drug x Time interaction, which indicated that the DMN connectivity between the two resting-state segments did not differ.

Figures 3B–D show a schematic 3D overview of the pairwise functional architecture of the DMN (sagittal view in **Fig. 3B**, transverse view in **Fig. 3C** and tilted sagittal view in **Fig. 3D**), with the DMN regions presented as blue orbs (for visual display purposes, orbs of 10 mm radius replaced actual ROIs at their center coordinates) and the functional connections as grey or red beams. Functional connections that showed a significant drug-related difference are marked in red. Note that the connections do not imply anatomical connectivity, or directed or conditional influences between regions.

Regional DMN Connectivity and Alertness

To investigate if regional functional connectivity contributed to self-reported alertness of the Bond and Lader VAS scale, we correlated the alertness ratings with the functional connectivity values of the seven connections. Alertness ratings and connectivity coefficients of escitalopram and placebo were averaged for each participant before correlation analysis. Decreased alertness correlated significantly with decreased posterior cingulate-parietal connectivity (PCC-RIPC: r = 0.78, P = 0.007; see **Fig. 4A**), and marginally with decreased hippocampal-parietal connectivity (LIPC-RHPC: r = 0.58, P = 0.08; see **Fig. 4B**). Thus, self-report level of alertness covaried with intrinsic DMN connectivity.

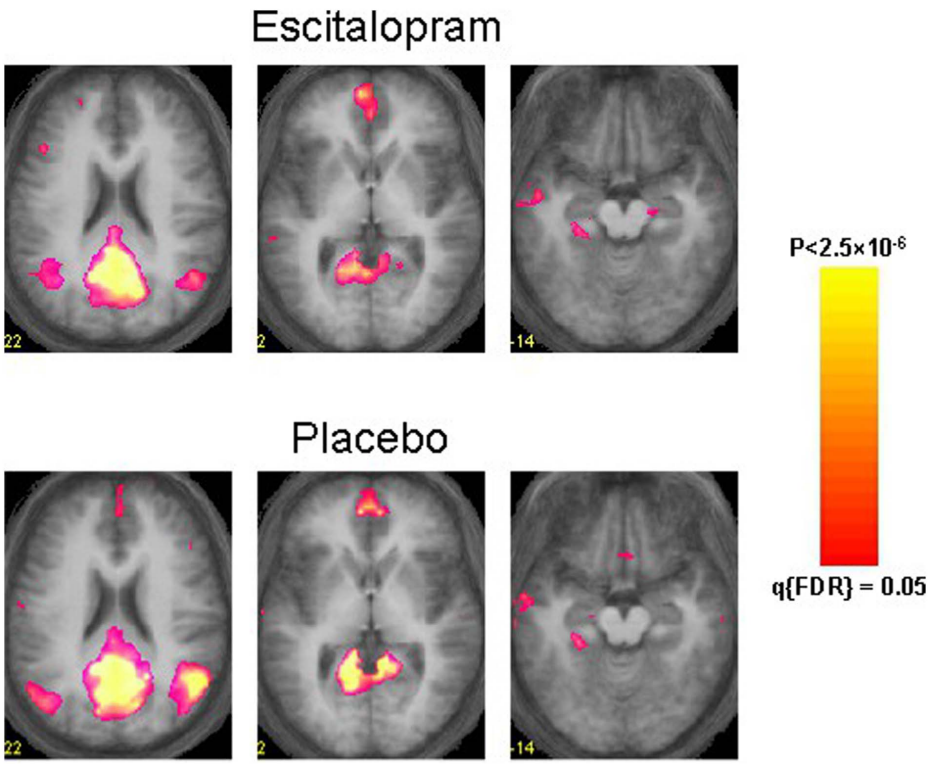

Figure 1. Default-mode networks after escitalopram (upper row) and placebo administration (bottom row). The figure shows three transverse slices (Talairach-Z coordinates 22, 2 and −14) of ICA-derived functional connectivity maps of the DMN superimposed on the anatomical average of the participants. The left hemisphere is depicted on the left side of each image.
doi:10.1371/journal.pone.0068355.g001

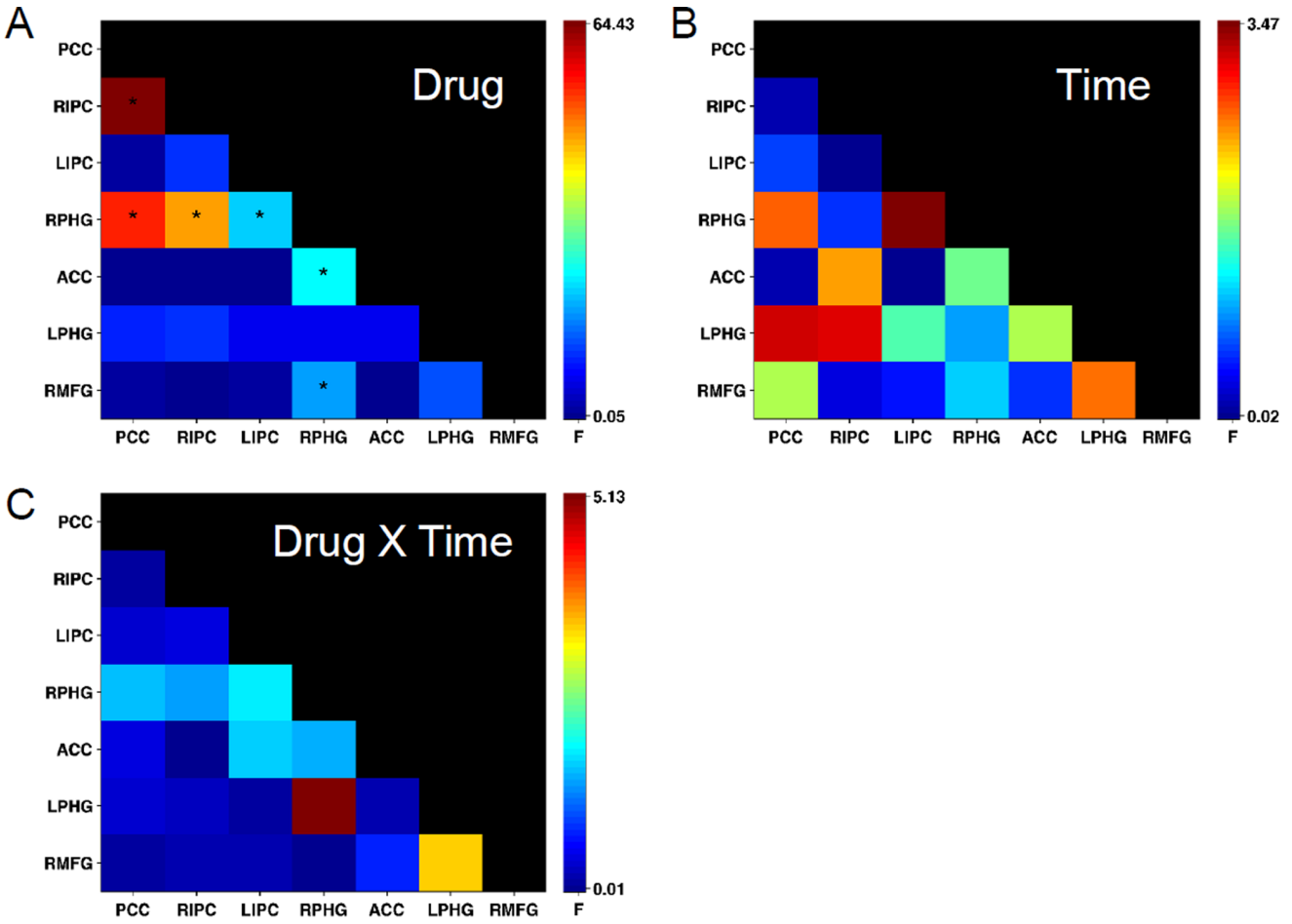

Figure 2. ROI-based RMANOVA results. Each panel depicts the color-coded RMANOVA F-values of the pairwise ROI functional connections for factors Drug (A), Time (B) and Drug x Time (C). Repetitive values in the ROI connections matrix are replaced with black. Degrees of freedom for plotted F-values are 1 and 9 in all cases. Asterisks mark ROI connections with significant results at q(FDR) = 0.05.
doi:10.1371/journal.pone.0068355.g002

Discussion

In this study we investigated if the SSRI escitalopram affected functional connectivity of the DMN during resting-state fMRI measurements. In both pharmacological conditions the DMN contained areas that have been reported in previous resting-state studies [1,2,4,5]. Escitalopram showed decreased regional pairwise connectivity between frontal, parietal and temporal regions, including hippocampus, parietal cortex and ventromedial cortex. These effects were found in two resting-state segments of the same individuals, suggesting that these effects are reliable and stable over time. We interpret these findings as evidence that escitalopram altered intrinsic DMN functional connectivity

Table 2. ROI connection details.

	RS1				RS2			
Conn	**Escit**	**Plac**	**T**	**P**	**Escit**	**Plac**	**T**	**P**
PCC-RIPC	.98	1.30	−3.7	.005	1.06	1.32	−4.0	.003
PCC-RPHC	.27	.73	−4.7	.001	.32	.82	−7.6	<.001
RIPC-RPHC	.21	.60	−3.4	.008	.20	.68	−8.5	<.001
LIPC-RPHC	.17	.60	−4.2	.002	.24	.63	−4.6	.001
RPHC-ACC	.14	.40	−2.5	.037	.18	.48	−6.0	<.001
RPHC-RMFG	.12	.43	−3.6	.006	.25	.43	−2.2	0.058

For each significant pairwise connection (Conn) the average connectivity values after Escitalopram (Escit) and Placebo (Plac) administration are shown, together with the paired-sample T-test statistics (degrees of freedom = 9), for both resting states RS1 and RS2. Abbreviations, see main text.
doi:10.1371/journal.pone.0068355.t002

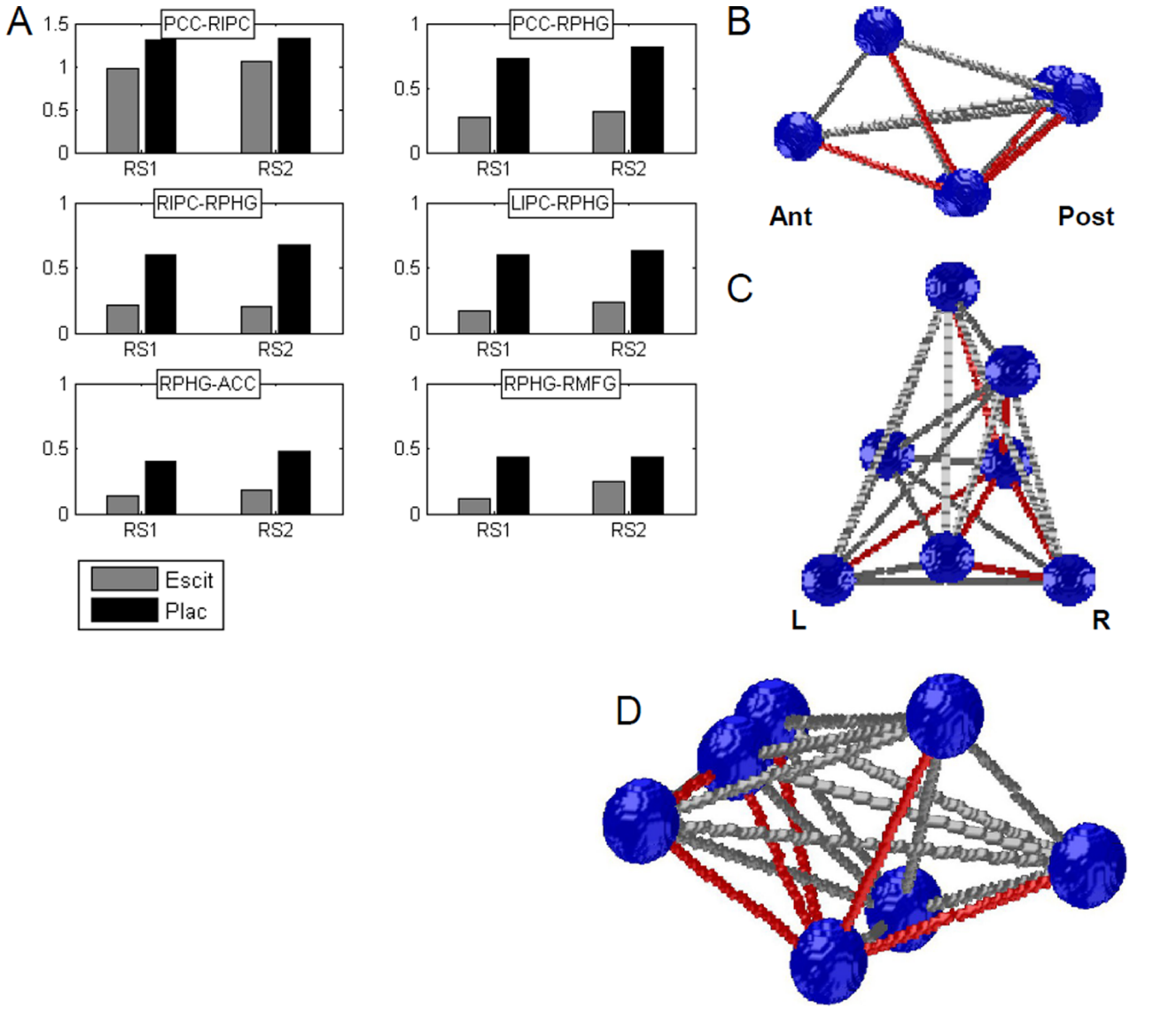

Figure 3. Escitalopram-induced changes in DMN functional connectivity. A: Bars show means of functional connectivity values (Fisher's Z normalized correlation coefficients) as a function of drug condition, and for each resting-state segment, for each of the six connections that were found significant after RMANOVA testing. Grey bars represent connectivity after Escitalopram administration, black bars after Placebo. B-D: Schematic 3D display of the DMN ROIs and their pairwise functional connections. ROIs are displayed as blue orbs (radius = 10 mm), significant connections are displayed as red beams connecting the orbs, non-significant connections are shown as grey beams. B: Lateral view (sagittal; left side is anterior). C: Top view (transverse; left side is left). D: Tilted side view.
doi:10.1371/journal.pone.0068355.g003

through the modulation of the functionality of the serotonergic system in the brain.

Our results fit with previous reports of regional changes in brain activity after serotonergic challenge. In a pharmacological challenge PET study, Mann et al. [30] administered the SSRI fenfluramine to healthy participants and found increased and decreased activity in respectively the ACC and PCC, compared to placebo. Geday et al. [68] showed in a pharmacological PET study decreased ACC activity after citalopram administration. Further, several fMRI studies showed decreased task-related activity in medial cortical, hippocampal, thalamic and cerebellar regions after SSRI administration [33,34,69,70]. In contrast, McKie et al. [29] used citalopram in a pharmacological challenge fMRI study and found increased activity in the subgenual part of the ACC, medial thalamus and hippocampus. These changes in SSRI-induced regional activity changes suggest that functional coupling between these and other areas may be reduced after serotonergic challenge. A recent report of decreased functional coupling between ACC and PCC after intake of the psychedelic psilocybin [38] lends further support to this suggestion, because the effects of psychedelic compounds may be initiated by stimulation of 5-HT receptors [39,71].

Findings from receptor mapping studies provide further support for the suggestion that escitalopram-related changes to DMN functional connectivity were based on altered serotonergic functioning. Receptor mapping studies in rodent and non-human primates showed that serotonergic afferents project to multiple regions of the limbic system, which include anterior and posterior portions of the cingulate cortex [72,73] and hippocampus [42,74]. A rat ph-fMRI study showed increased functional coupling

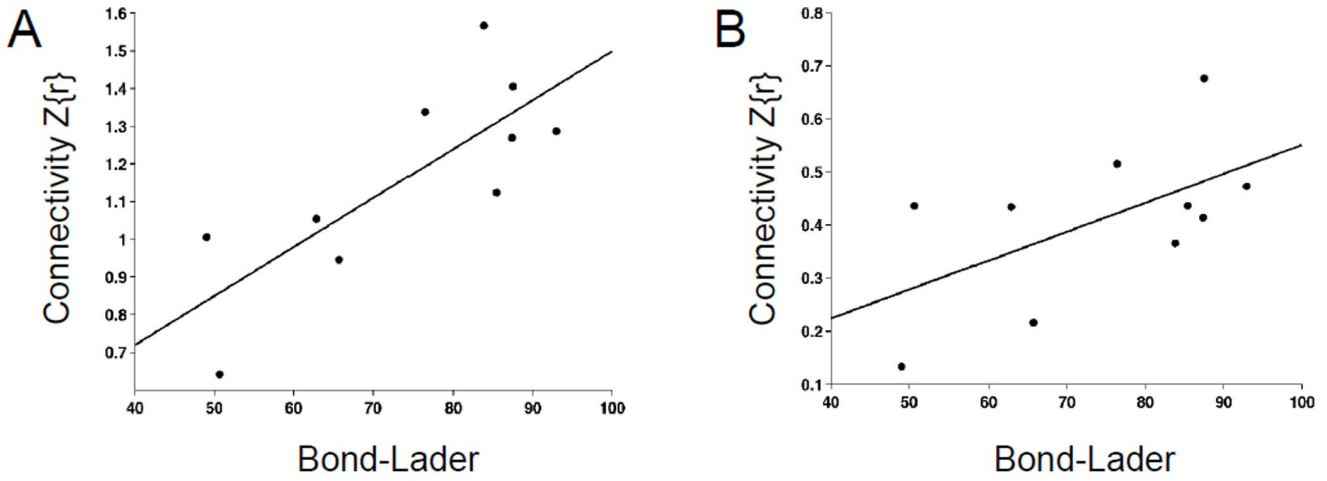

Figure 4. Scatterplots. Shown are the scatterplots of functional connectivity between PCC and RIPC (A), and between LIPC and RPHC (B) as a function of alertness ratings of the Bond and Lader VAS scale. Each data point represents one participant. A regression line (least squares fit) is drawn through the data points in each plot. Functional connectivity and VAS rating values are the average of the Escitalopram and Placebo conditions.
doi:10.1371/journal.pone.0068355.g004

amongst sub-cortical regions that were part of serotonin pathways, including raphe nuclei, hippocampus and thalamus in the rat brain after fluoxetine challenge [75]. Finally, neurophysiological studies in animals show that the results of our and other neuroimaging studies are likely associated with changes in metabolic demands as a consequence of altered serotonin levels, rather than with vasodynamics unrelated to neurophysiology [30,75,76]. Of potential relevance here are reports that the neurophysiological basis of the fMRI signal may capitalize more on synaptic activity, rather than on neuronal spike or firing rates [77–79], which could indicate that serotonergic effects on neurophysiology occur most strongly at synaptic connection sites.

Our results also show that escitalopram-induced changes in DMN functional organization may have contributed to decreased alertness or vigilance. This finding fits with the DMN's putative involvement in ongoing monitoring of internal representations when the brain is not engaged in a stimulus-driven task [80,81]. This association may be relevant for task performance, in which changes in vigilance or sustained attention can influence task-related processing. Reduced DMN deactivation during vigilance tasks may indicate that the DMN is involved in reallocating processing resources away from the task at hand [9,82,83]. Furthermore, several studies have shown that administration of SSRIs may impair vigilance in healthy participants [43,84,85], which further supports our interpretation that escitalopram altered DMN functionality through altered serotonergic functioning.

Our findings could be relevant for understanding the neurobiological mechanism of the DMN's contribution to cognition. For example, there is growing evidence that posterior regions of the DMN are involved in (episodic) memory processing [4,10,12,86,87]. Previous studies showed that decreased serotonin levels may impair long-term memory performance in healthy participants [44,45], and increased 5-HT levels may improve [88] as well as impair memory performance [84,89]. A recent placebo-controlled ph-fMRI study in which 3,4-methylenedioxy-methamphetamine (MDMA) was administered to healthy participants showed reduced deactivation in inferior parietal areas, compared to placebo, which correlated with increased prospective memory failure [90]. These authors concluded that reduced activation in inferior parietal cortex may have resulted from increased serotonergic availability after acute MDMA administration, thereby impairing memory performance.

Our study focused primarily on the functional connectivity of the DMN, but it is possible that escitalopram affected other resting-state networks as well. The intrinsic functional architecture of the human brain comprises multiple neural networks [91,92]. Serotonergic afferents project to many different cortical and subcortical areas beyond DMN regions [42,93]. Serotonergic activity is important for synaptic plasticity and functional organization in the mammalian primary visual cortex [79,94,95], and may play a role in reorganization of neural networks of the motor system [69,96]. At the same time, ph-fMRI studies provide little evidence for serotonergic effects in lateral prefrontal and posterior parietal cortex [97], which are commonly associated with executive control and attentional task performance [3,98]. Thus, it would be of interest to investigate in a more exploratory fashion which resting-state networks escitalopram affects. However, this approach is beyond the scope of the current paper.

A few issues deserve consideration. The small sample size, comparable to previous ph-fMRI studies [97], could have underpowered the map-level analysis. However, our findings indicate that a regional analysis may be more appropriate than a voxel-by-voxel analysis in possible low-power cases. An important methodological consideration in resting-state fMRI is the possible confounding effect of physiological responses, such as cardiac or respiratory rate, to measurements of intrinsic brain activity [62,63,99], which may be further increased in pharmacological challenge studies. Several studies did not find significant differences in heart rate after escitalopram administration, compared to placebo [100,101], although small decreases have been reported [102]. We aimed to minimize possible influences to the functional connectivity estimates in several ways. Spatial ICA can reliably separate functional connectivity maps of putative neurophysiological sources from physiological responses, such as respiratory or pulse rate, and other signal artifacts [62,103–105]. We also removed signals from ventricular and white matter areas from the functional connectivity estimates [62], and restricted our analysis to signal fluctuations occurring below 0.1 Hz. A second methodological issue concerns the application of dual-regression analysis to different segments of the data. Using the sICA solution of an

aggregated dataset in the dual-regression approach indirectly imposes a desirable data reduction step that is similar to group-based PCA [50]. However, this also introduces circularity or re-usage of the data in the analysis pipeline. In our study, we used the sICA solution of one segment of the data to explain the same and another, independent segment of the functional timeseries, and showed that the functional connectivity results did not differ between the two segments. Thirdly, the two resting-state measurements were extracted from a larger dataset in which participants performed a vigilance task in-between the resting states. There are some indications that task performance may alter the functional architecture of *post-task* resting-state networks [26,106–108]. However, we found no evidence for an effect of the vigilance task on global or local intrinsic DMN connectivity, indicating that the task did not bias our main results. Finally, we did not obtain resting-state baseline measurements prior to experimental manipulation.

In conclusion, escitalopram administration to healthy participants decreased functional connectivity of medial frontal, parietal and hippocampal regions within the DMN. These regional changes appear in line with reported behavioral and functional imaging results after administration of serotonergic agents. We propose that resting-state ph-fMRI is a valuable neuroimaging tool to further investigate the intrinsic functional architecture of the brain in healthy and clinical populations.

Author Contributions

Conceived and designed the experiments: VV MW KPCK JGR EF. Performed the experiments: MW KPCK. Analyzed the data: VV EF. Contributed reagents/materials/analysis tools: JGR. Wrote the paper: VV JGR EF.

References

1. Greicius MD, Krasnow B, Reiss AL, Menon V (2003) Functional connectivity in the resting brain: a network analysis of the default mode hypothesis. Proceedings of the National Academy of Sciences U S A 100: 253–258.
2. Fransson P (2005) Spontaneous low-frequency BOLD signal fluctuations: an fMRI investigation of the resting-state default mode of brain function hypothesis. Human Brain Mapping 26: 15–29.
3. Fox MD, Snyder AZ, Vincent JL, Corbetta M, Van Essen DC, et al. (2005) The human brain is intrinsically organized into dynamic, anticorrelated functional networks. Proceedings of the National Academy of Sciences U S A 102: 9673–9678.
4. Vincent JL, Snyder AZ, Fox MD, Shannon BJ, Andrews JR, et al. (2006) Coherent spontaneous activity identifies a hippocampal-parietal memory network. Journal of Neurophysiology 96: 3517–3531.
5. Raichle ME, MacLeod AM, Snyder AZ, Powers WJ, Gusnard DA, et al. (2001) A default mode of brain function. Proceedings of the National Academy of Sciences U S A 98: 676–682.
6. Gusnard DA, Akbudak E, Shulman GL, Raichle ME (2001) Medial prefrontal cortex and self-referential mental activity: relation to a default mode of brain function. Proceedings of the National Academy of Sciences U S A 98: 4259–4264.
7. Schilbach L, Eickhoff SB, Rotarska-Jagiela A, Fink GR, Vogeley K (2008) Minds at rest? Social cognition as the default mode of cognizing and its putative relationship to the "default system" of the brain. Consciousness and Cognition 17: 457–467.
8. Jardri R, Pins D, Bubrovszky M, Despretz P, Pruvo J-P, et al. (2007) Self awareness and speech processing: an fMRI study. NeuroImage 35: 1645–1653.
9. Mason MF, Norton MI, Van Horn JD, Wegner DM, Grafton ST, et al. (2007) Wandering minds: the default network and stimulus-independent thought. Science 315: 393–395.
10. Hampson M, Driesen NR, Skudlarski P, Gore JC, Constable RT (2006) Brain connectivity related to working memory performance. Journal of Neuroscience 26: 13338–13343.
11. McKiernan KA, Kaufman JN, Kucera-Thompson J, Binder JR (2003) A parametric manipulation of factors affecting task-induced deactivation in functional neuroimaging. Journal of Cognitive Neuroscience 15: 394–408.
12. Spreng RN, Mar RA, Kim ASN (2009) The common neural basis of autobiographical memory, prospection, navigation, theory of mind, and the default mode: a quantitative meta-analysis. Journal of Cognitive Neuroscience 21: 489–510.
13. Van de Ven V, Bledowski C, Prvulovic D, Goebel R, Formisano E, et al. (2008) Visual target modulation of functional connectivity networks revealed by self-organizing group ICA. Human Brain Mapping 29: 1450–1461.
14. Greicius MD, Srivastava G, Reiss AL, Menon V (2004) Default-mode network activity distinguishes Alzheimer's disease from healthy aging: evidence from functional MRI. Proceedings of the National Academy of Sciences U S A 101: 4637–4642.
15. Rombouts SARB, Barkhof F, Goekoop R, Stam CJ, Scheltens P (2005) Altered resting state networks in mild cognitive impairment and mild Alzheimer's disease: an fMRI study. Human Brain Mapping 26: 231–239.
16. Buckner RL, Snyder AZ, Shannon BJ, LaRossa G, Sachs R, et al. (2005) Molecular, structural, and functional characterization of Alzheimer's disease: evidence for a relationship between default activity, amyloid, and memory. Journal of Neuroscience 25: 7709–7717.
17. Greicius MD, Flores BH, Menon V, Glover GH, Solvason HB, et al. (2007) Resting-state functional connectivity in major depression: abnormally increased contributions from subgenual cingulate cortex and thalamus. Biological Psychiatry 62: 429–437.
18. Sheline YI, Price JL, Yan Z, Mintun MA (2010) Resting-state functional MRI in depression unmasks increased connectivity between networks via the dorsal nexus. Proceedings of the National Academy of Sciences U S A 107: 11020–11025.
19. Wible CG, Preus AP, Hashimoto R (2009) A Cognitive Neuroscience View of Schizophrenic Symptoms: Abnormal Activation of a System for Social Perception and Communication. Brain Imaging and Behavior 3: 85–110.
20. Van de Ven V (2012) Brain functioning when the voices are silent - Aberrant default-mode and disrupted connectivity in auditory verbal hallucinations. In: Jardri R, Cachia A, Thomas P, Pins D, editors. The neuroscience of hallucinations. New York, NY: Springer. 393–415.
21. Damoiseaux JS, Rombouts SARB, Barkhof F, Scheltens P, Stam CJ, et al. (2006) Consistent resting-state networks across healthy subjects. Proceedings of the National Academy of Sciences U S A 103: 13848–13853.
22. Van de Ven VG, Formisano E, Prvulovic D, Roeder CH, Linden DEJ (2004) Functional connectivity as revealed by spatial independent component analysis of fMRI measurements during rest. Human Brain Mapping 22: 165–178.
23. Schölvinck ML, Maier A, Ye FQ, Duyn JH, Leopold DA (2010) Neural basis of global resting-state fMRI activity. Proceedings of the National Academy of Sciences U S A 107: 10238–10243.
24. Shmuel A, Leopold DA (2008) Neuronal correlates of spontaneous fluctuations in fMRI signals in monkey visual cortex: Implications for functional connectivity at rest. Human Brain Mapping 29: 751–761.
25. Mantini D, Perrucci MG, Del Gratta C, Romani GL, Corbetta M (2007) Electrophysiological signatures of resting state networks in the human brain. Proceedings of the National Academy of Sciences U S A 104: 13170–13175.
26. Tambini A, Ketz N, Davachi L (2010) Enhanced brain correlations during rest are related to memory for recent experiences. Neuron 65: 280–290.
27. Fox MD, Snyder AZ, Vincent JL, Raichle ME (2007) Intrinsic fluctuations within cortical systems account for intertrial variability in human behavior. Neuron 56: 171–184.
28. De Weerd P, Reithler J, Van de Ven V, Been M, Jacobs C, et al. (2012) Posttraining Transcranial Magnetic Stimulation of Striate Cortex Disrupts Consolidation Early in Visual Skill Learning. Journal of Neuroscience 32: 1981–1988.
29. McKie S, Del-Ben C, Elliott R, Williams S, Del Vai N, et al. (2005) Neuronal effects of acute citalopram detected by pharmacoMRI. Psychopharmacology 180: 680–686.
30. Mann JJ, Malone KM, Diehl DJ, Perel J, Nichols TE, et al. (1996) Positron emission tomographic imaging of serotonin activation effects on prefrontal cortex in healthy volunteers. Journal of Cerebral Blood Flow and Metabolism 16: 418–426.
31. Del-Ben CM, Deakin JFW, McKie S, Delvai NA, Williams SR, et al. (2005) The effect of citalopram pretreatment on neuronal responses to neuropsychological tasks in normal volunteers: an FMRI study. Neuropsychopharmacology 30: 1724–1734.
32. Loubinoux I, Pariente J, Boulanouar K, Carel C, Manelfe C, et al. (2002) A single dose of the serotonin neurotransmission agonist paroxetine enhances motor output: double-blind, placebo-controlled, fMRI study in healthy subjects. Neuroimage 15: 26–36.
33. Rose EJ, Simonotto E, Spencer EP, Ebmeier KP (2006) The effects of escitalopram on working memory and brain activity in healthy adults during performance of the n-back task. Psychopharmacology 185: 339–347.
34. Wingen M, Kuypers KPC, Van de Ven V, Formisano E, Ramaekers JG (2008) Sustained attention and serotonin: a pharmaco-fMRI study. Human Psychopharmacology: Clinical and Experimental 23: 221–230.

35. Esposito F, Pignataro G, Di Renzo G, Spinali A, Paccone A, et al. (2010) Alcohol increases spontaneous BOLD signal fluctuations in the visual network. NeuroImage 53: 534–543.
36. Khalili-Mahani N, Zoethout RMW, Beckmann CF, Baerends E, De Kam ML, et al. (2011) Effects of morphine and alcohol on functional brain connectivity during ''resting state'':A placebo-controlled crossover study in healthy young men. Human Brain Mapping 000.
37. Kelly C, De Zubicaray G, Di Martino A, Copland DA, Reiss PT, et al. (2009) L-dopa modulates functional connectivity in striatal cognitive and motor networks: a double-blind placebo-controlled study. Journal of Neuroscience 29: 7364–7378.
38. Carhart-Harris RL, Erritzoe D, Williams T, Stone JM, Reed LJ, et al. (2012) Neural correlates of the psychedelic state as determined by fMRI studies with psilocybin. Proceedings of the National Academy of Sciences U S A 109: 2138–2143.
39. Nichols DE (2004) Hallucinogens. Pharmacology & Therapeutics 101: 131–181.
40. Northoff G, Walter M, Schulte RF, Beck J, Dydak U, et al. (2007) GABA concentrations in the human anterior cingulate cortex predict negative BOLD responses in fMRI. Nature Neuroscience 10: 1515–1517.
41. Meeter M, Talamini L, Schmitt JAJ, Riedel WJ (2006) Effects of 5-HT on memory and the hippocampus: model and data. Neuropsychopharmacology 31: 712–720.
42. Meneses A (1999) 5-HT system and cognition. Neuroscience & Biobehavioral Reviews 23: 1111–1125.
43. Schmitt JAJ, Wingen M, Ramaekers JG, Evers EAT, Riedel WJ (2006) Serotonin and human cognitive performance. Current Pharmaceutical Design 12: 2473–2486.
44. Riedel WJ, Klaassen T, Deutz NE, Van Someren A, Van Praag HM (1999) Tryptophan depletion in normal volunteers produces selective impairment in memory consolidation. Psychopharmacology 141: 362–369.
45. Sobczak S, Riedel WJ, Booij I, Aan Het Rot M, Deutz NEP, et al. (2002) Cognition following acute tryptophan depletion: difference between first-degree relatives of bipolar disorder patients and matched healthy control volunteers. Psychological Medicine 32: 503–515.
46. Meltzer CC, Smith G, DeKosky ST, Pollock BG, Mathis CA, et al. (1998) Serotonin in aging, late-life depression, and Alzheimer's disease: the emerging role of functional imaging. Neuropsychopharmacology 18: 407–430.
47. Tamminga CA (2006) The neurobiology of cognition in schizophrenia. Journal of Clinical Psychiatry 67: e11.
48. Esposito F, Aragri A, Pesaresi I, Cirillo S, Tedeschi G, et al. (2008) Independent component model of the default-mode brain function: combining individual-level and population-level analyses in resting-state fMRI. Magnetic resonance imaging 26: 905–913.
49. Smith SM (2012) The future of FMRI connectivity. NeuroImage 62: 1257–1266.
50. Erhardt EB, Rachakonda S, Bedrick EJ, Allen EA, Adali T, et al. (2011) Comparison of multi-subject ICA methods for analysis of fMRI data. Human Brain Mapping 32: 2075–2095.
51. McKeown MJ, Makeig S, Brown GG, Jung TP, Kindermann SS, et al. (1998) Analysis of fMRI data by blind separation into independent spatial components. Human Brain Mapping 6: 160–188.
52. Calhoun VD, Adali T, Pearlson GD, Pekar JJ (2001) A Method for Making Group Inferences from Functional MRI Data Using Independent Component Analysis. Human Brain Mapping 151: 140–151.
53. Aronson S, Delgado P (2004) Escitalopram. Drugs Today 40: 121–131.
54. Bond A, Lader M (1974) The use of analogue scales in rating subjective feelings. British Journal of Medical Psychology 47: 211–218.
55. Goebel R, Esposito F, Formisano E (2006) Analysis of functional image analysis contest (FIAC) data with brainvoyager QX: From single-subject to cortically aligned group general linear model analysis and self-organizing group independent component analysis. Human Brain Mapping 27: 392–401.
56. Talairach J, Tournoux P (1988) Co-planar stereotaxic atlas of the human brain. New York: Thieme Medical.
57. Hyvarinen A, Oja E (1997) A Fast Fixed-Point Algorithm for Independent Component Analysis. Neural Computation 9: 1483–1492.
58. Formisano E, Esposito F, Di Salle F, Goebel R (2004) Cortex-based independent component analysis of fMRI time series. Magnetic Resonance Imaging 22: 1493–1504.
59. Svensén M, Kruggel F, Benali H (2002) ICA of fMRI Group Study Data. NeuroImage 16: 551–563.
60. Abou Elseoud A, Littow H, Remes J, Starck T, Nikkinen J, et al. (2011) Group-ICA Model Order Highlights Patterns of Functional Brain Connectivity. Frontiers in Systems Neuroscience 5: 37.
61. Zuo X-N, Kelly C, Adelstein JS, Klein DF, Castellanos FX, et al. (2010) Reliable intrinsic connectivity networks: test-retest evaluation using ICA and dual regression approach. NeuroImage 49: 2163–2177.
62. Birn RM, Murphy K, Handwerker D a, Bandettini P a (2009) fMRI in the presence of task-correlated breathing variations. NeuroImage 47: 1092–1104.
63. Birn RM, Diamond JB, Smith MA, Bandettini P a (2006) Separating respiratory-variation-related fluctuations from neuronal-activity-related fluctuations in fMRI. Neuroimage 31: 1536–1548.
64. Rombouts S a RB, Stam CJ, Kuijer JP a, Scheltens P, Barkhof F (2003) Identifying confounds to increase specificity during a ''no task condition''. Evidence for hippocampal connectivity using fMRI. NeuroImage 20: 1236–1245.
65. Trujillo-Ortiz A, Hernandez-Walls R, Trujillo-Perez FA (2010) RMAOV33: Three-way Analysis of Variance With Repeated Measures on Three Factors Test. A MATLAB file. Matlab Central Fileexchange.
66. Genovese CR, Lazar NA, Nichols T (2002) Thresholding of statistical maps in functional neuroimaging using the false discovery rate. Neuroimage 15: 870–878.
67. Forman SD, Cohen JD, Fitzgerald M, Eddy WF, Mintun MA, et al. (1995) Improved assessment of significant activation in functional magnetic resonance imaging (fMRI): use of a cluster-size threshold. Magnetic Resonance in Medicine 33: 636–647.
68. Geday J, Hermansen F, Rosenberg R, Smith DF (2005) Serotonin modulation of cerebral blood flow measured with positron emission tomography (PET) in humans. Synapse 55: 224–229.
69. Loubinoux I, Tombari D, Pariente J, Gerdelat-Mas A, Franceries X, et al. (2005) Modulation of behavior and cortical motor activity in healthy subjects by a chronic administration of a serotonin enhancer. Neuroimage 27: 299–313.
70. Harmer CJ, Mackay CE, Reid CB, Cowen PJ, Goodwin GM (2006) Antidepressant drug treatment modifies the neural processing of nonconscious threat cues. Biological Psychiatry 59: 816–820.
71. Aghajanian GK, Marek GJ (1999) Serotonin and hallucinogens. Neuropsychopharmacology 21: 16S–23S.
72. Bozkurt A, Zilles K, Schleicher A, Kamper L, Arigita EJS, et al. (2005) Distributions of transmitter receptors in the macaque cingulate cortex. Neuroimage 25: 219–229.
73. Puig MV, Santana N, Celada P, Mengod G, Artigas F (2004) In vivo excitation of GABA interneurons in the medial prefrontal cortex through 5-HT3 receptors. Cerebral Cortex 14: 1365–1375.
74. Brady CA, Dover TJ, Massoura AN, Princivalle AP, Hope AG, et al. (2007) Identification of 5-HT3A and 5-HT3B receptor subunits in human hippocampus. Neuropharmacology 52: 1284–1290.
75. Schwarz AJ, Gozzi A, Reese T, Bifone A (2007) In vivo mapping of functional connectivity in neurotransmitter systems using pharmacological MRI. NeuroImage 34: 1627–1636.
76. McBean DE, Ritchie IM, Olverman HJ, Kelly PA (1999) Effects of the specific serotonin reuptake inhibitor, citalopram, upon local cerebral blood flow and glucose utilisation in the rat. Brain Research 847: 80–84.
77. Logothetis NK, Pauls J, Augath M, Trinath T, Oeltermann A (2001) Neurophysiological investigation of the basis of the fMRI signal. Nature 412: 150–157.
78. Raichle ME, Mintun MA (2006) Brain work and brain imaging. Annual Review of Neuroscience 29: 449–476.
79. Rauch A, Rainer G, Logothetis NK (2008) The effect of a serotonin-induced dissociation between spiking and perisynaptic activity on BOLD functional MRI. Proceedings of the National Academy of Sciences U S A 105: 6759–6764.
80. Gusnard D, Raichle M (2001) Searching for a baseline: functional imaging and the resting human brain. Nature Reviews Neuroscience 2: 685–694.
81. Fox MD, Raichle ME (2007) Spontaneous fluctuations in brain activity observed with functional magnetic resonance imaging. Nature Reviews Neuroscience 8: 700–711.
82. Drummond SP, Bischoff-Grethe A, Dinges DF, Ayalon L, Mednick SC, et al. (2005) The neural basis of the psychomotor vigilance task. Sleep 28: 1059–1068.
83. Weissman DH, Roberts KC, Visscher KM, Woldorff MG (2006) The neural bases of momentary lapses in attention. Nature Neuroscience 9: 971–978.
84. Riedel WJ, Eikmans K, Heldens A, Schmitt JA (2005) Specific serotonergic reuptake inhibition impairs vigilance performance acutely and after subchronic treatment. Journal of Psychopharmacology 19: 12–20.
85. Ramaekers JG, Muntjewerff ND, O'Hanlon JF (1995) A comparative study of acute and subchronic effects of dothiepin, fluoxetine and placebo on psychomotor and actual driving performance. British Journal of Clinical Pharmacology 39: 397–404.
86. Sestieri C, Corbetta M, Romani GL, Shulman GL (2011) Episodic memory retrieval, parietal cortex, and the default mode network: functional and topographic analyses. Journal of Neuroscience 31: 4407–4420.
87. Esposito F, Bertolino A, Scarabino T, Latorre V, Blasi G, et al. (2006) Independent component model of the default-mode brain function: Assessing the impact of active thinking. Brain Research Bulletin 70: 263–269.
88. Harmer CJ, Bhagwagar Z, Cowen PJ, Goodwin GM (2002) Acute administration of citalopram facilitates memory consolidation in healthy volunteers. Psychopharmacology 163: 106–110.
89. Wingen M, Kuypers KP, Ramaekers JG (2007) Selective verbal and spatial memory impairment after 5-HT1A and 5-HT2A receptor blockade in healthy volunteers pre-treated with an SSRI. Journal of Psychopharmacology 21: 477–485.
90. Ramaekers JG, Kuypers KPC, Wingen M, Heinecke A, Formisano E (2009) Involvement of inferior parietal lobules in prospective memory impairment during acute MDMA (ecstasy) intoxication: an event-related fMRI study. Neuropsychopharmacology 34: 1641–1648.
91. Van den Heuvel MP, Hulshoff Pol HE (2010) Exploring the brain network: a review on resting-state fMRI functional connectivity. European Neuropsychopharmacology 20: 519–534.

92. Auer DP (2008) Spontaneous low-frequency blood oxygenation level-dependent fluctuations and functional connectivity analysis of the "resting" brain. Magnetic Resonance Imaging 26: 1055–1064.
93. Wilson MA, Molliver ME (1991) The organization of serotonergic projections to cerebral cortex in primates: regional distribution of axon terminals. Neuroscience 44: 537–553.
94. Maya Vetencourt JF, Sale A, Viegi A, Baroncelli L, De Pasquale R, et al. (2008) The antidepressant fluoxetine restores plasticity in the adult visual cortex. Science 320: 385–388.
95. Roerig B, Katz LC, Carolina N (1997) Modulation of intrinsic circuits by serotonin 5-HT3 receptors in developing ferret visual cortex. Journal of Neuroscience 17: 8324–8338.
96. Pariente J, Loubinoux I, Carel C, Albucher JF, Leger A, et al. (2001) Fluoxetine modulates motor performance and cerebral activation of patients recovering from stroke. Annals of Neurology 50: 718–729.
97. Anderson IM, McKie S, Elliott R, Williams SR, Deakin JFW (2008) Assessing human 5-HT function in vivo with pharmacoMRI. Neuropharmacology 55: 1029–1037.
98. Seeley WW, Menon V, Schatzberg AF, Keller J, Glover GH, et al. (2007) Dissociable intrinsic connectivity networks for salience processing and executive control. Journal of Neuroscience 27: 2349–2356.
99. Shmueli K, Van Gelderen P, De Zwart JA, Horovitz SG, Fukunaga M, et al. (2007) Low-frequency fluctuations in the cardiac rate as a source of variance in the resting-state fMRI BOLD signal. Neuroimage 38: 306–320.
100. Penttila J, Syvalahti E, Hinkka S, Kuusela T, Scheinin H (2001) The effects of amitriptyline, citalopram and reboxetine on autonomic nervous system. A randomised placebo-controlled study on healthy volunteers. Psychopharmacology 154: 343–349.
101. Seifritz E, Baumann P, Muller MJ, Annen O, Amey M, et al. (1996) Neuroendocrine effects of a 20-mg citalopram infusion in healthy males. A placebo-controlled evaluation of citalopram as 5-HT function probe. Neuropsychopharmacology 14: 253–263.
102. Rasmussen SL, Overø KF, Tanghøj P (1999) Cardiac safety of citalopram: prospective trials and retrospective analyses. Journal of Clinical Psychopharmacology 19: 407–415.
103. Kiviniemi V, Kantola JH, Jauhiainen J, Hyvarinen A, Tervonen O (2003) Independent component analysis of nondeterministic fMRI signal sources. Neuroimage 19: 253–260.
104. Liao R, McKeown MJ, Krolik JL (2006) Isolation and minimization of head motion-induced signal variations in fMRI data using independent component analysis. Magnetic Resonance in Medicine 55: 1396–1413.
105. Thomas CG, Harshman R, Menon RS (2002) Noise reduction in BOLD-based fMRI using component analysis. Neuroimage 17: 1521–1537.
106. Sidtis JJ, Strother SC, Rottenberg DA (2004) The effect of set on the resting state in functional imaging: a role for the striatum? NeuroImage 22: 1407–1413.
107. Hasson U, Nusbaum HC, Small SL (2009) Task-dependent organization of brain regions active during rest. Proceedings of the National Academy of Sciences U S A 106: 10841–10846.
108. Waites AB, Stanislavsky A, Abbott DF, Jackson GD (2005) Effect of prior cognitive state on resting state networks measured with functional connectivity. Human Brain Mapping 24: 59–68.